

Dynamics and Instability of Electron Phase-Space Tubes

D. L. Newman,* M. V. Goldman, M. Spector, and F. Perez

CIPS, University of Colorado, Boulder, Colorado 80309-0390

(Received 16 August 2000)

Two-dimensional simulations of beam-driven turbulence in the auroral ionosphere have shown the formation and instability of phase-space tubes. These tubes are a generalization of electron phase-space holes in a one-dimensional plasma. In a strongly magnetized plasma, such tubes vibrate at frequencies below the bounce frequency of the trapping potential. A theory for these vibrations yields quantitative agreement with kinetic simulations. Furthermore, the theory predicts that the vibrations can become unstable when resonantly coupled to electrostatic whistlers—also in agreement with simulations.

DOI: 10.1103/PhysRevLett.86.1239

PACS numbers: 52.35.Sb, 52.35.Mw, 52.65.Cc

Observations of bipolar electric field structures in Earth's auroral ionosphere [1] have been interpreted as signatures of electron phase-space holes. In a 1D plasma, such holes have been modeled [2] as stationary Bernstein-Green-Kruskal (BGK) solutions of the Vlasov and Poisson equations [3]. The stability of generalized holes in higher dimensions, however, is a subject of ongoing study.

Recent two-dimensional particle simulations [4] of the two-stream instability in a highly magnetized ($\Omega_e > \omega_e$) plasma show the formation of phase-space tubes (i.e., holes extended in the direction perpendicular to \mathbf{B}). The bipolar electric fields associated with these tubes are in quantitative agreement with typical fast auroral snapshot (FAST) satellite observations [1,4], which exhibit a range of amplitudes and spatial sizes [2]. After several hundred ω_e^{-1} , but before the ion response becomes important [5], these tubes are observed to break up simultaneously with the appearance of electrostatic whistler waves (i.e., magnetically modified Langmuir waves with dispersion $\omega_w/\omega_e \approx k_{\parallel}/k_{\perp} \ll 1$). Subsequent simulations [6] initialized with straight tubes revealed kink perturbations oscillating with a “vibration” frequency $\omega_v \approx \omega_w$, suggesting a resonant interaction between the tubes and whistlers.

In this Letter, we present a quantitative theory for both the vibrations of kinked tubes and the resonant interaction of the tube vibrations with electrostatic whistlers. The predictions of this theory are also compared to the results of magnetized 2D Vlasov simulations. Scaling laws based on an approximation to this theory are presented elsewhere [7].

The ordering of key frequencies in our analytical treatment is the same as in the two-stream simulations motivated by FAST observations in the auroral ionosphere:

$$\omega_r \approx \omega_v \approx \omega_w < \omega_b < \omega_e < \Omega_e, \quad (1)$$

where the real frequency of the instability is at ω_r , and ω_b is the characteristic “bounce” frequency of an electron trapped in the potential well of the bipolar field. The frequency ordering (1) distinguishes this instability from another recently discussed instability of phase-space tubes: Muschietti *et al.* [8] consider an instability in the regime

$\Omega_e < \omega_b$. The mechanism of Vetoulis and Oppenheim [9] is also inconsistent with frequency ordering (1) in that it predicts $\omega_r = \omega_b$ or integer multiples of ω_b .

We consider a two-dimensional (x - y) collisionless plasma with a uniform embedded magnetic field \mathbf{B} in the x direction. The electric field can be determined from the density via Poisson's equation

$$\mathbf{E} = -\nabla\phi, \quad \nabla^2\phi = -\rho \equiv n_e - 1, \quad (2)$$

where a uniform, static, neutralizing ion background is assumed. We note that an electron's potential energy is $-\phi$. Dimensionless units will be used throughout in which time is in units of ω_e^{-1} , velocity is in units of a characteristic velocity V (e.g., as in Fig. 1), distance is in units of an “effective” Debye length ($\lambda_e = V/\omega_e$), electron density is normalized to the ion density n_0 , and the electric field is normalized to $4\pi\lambda_en_0e$, where e is the electron charge in Gaussian units. We further simplify our model by neglecting the effect of electron motion perpendicular to \mathbf{B} for the low-frequency ($\omega \ll \Omega_e$) phenomena being considered. Previous 2D particle in cell (PIC) simulations in which all three electron velocity components were retained [6] revealed negligible differences in the formation and instability of electron phase-space tubes when Ω_e was increased from $5\omega_e$ to ∞ . These simulations support our neglect of perpendicular electron motion.

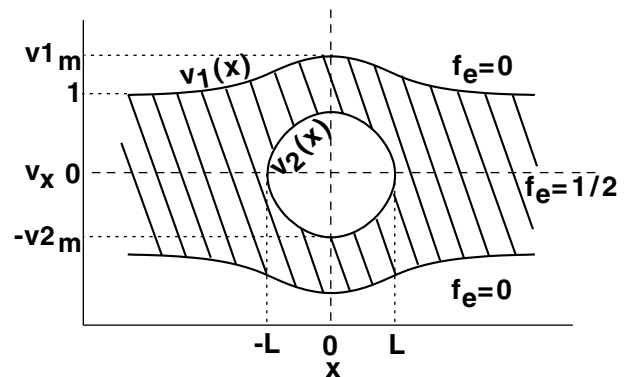


FIG. 1. Schematic of a waterbag BGK phase-space hole in which various values quantifying properties of the hole are defined. Velocities are normalized to $V \equiv v_1(\pm\infty)$.

The resulting Vlasov equation that governs the collisionless evolution of the phase-space distribution $f_e(x, v_x, y, t)$ is

$$(\partial_t + v_x \partial_x - E_x \partial_{v_x}) f_e(x, v_x, y, t) = 0. \quad (3)$$

Equation (3) can be interpreted as a system of parallel 1D Vlasov equations (spanning y) coupled via the parallel electric field $E_x(x, y)$, which is determined through the 2D Poisson equation (2). We refer to the coupled system as a “reduced” 2D Vlasov-Poisson system.

The tubes generated in our simulations of the two-stream instability were found to be surrounded by broad plateaus of near-constant phase-space density. Therefore, we have chosen for our model of an unperturbed phase-space tube a stationary BGK waterbag hole in x - v_x phase space [10] that has been extended uniformly in the y direction. Such a hole is shown in Fig. 1, in which key properties of the distribution are defined.

Numerical simulations based on the reduced Vlasov-Poisson equations (3) and (2) were used to study the evolution of our model phase-space tube in which a “kink” perturbation is imposed. The kink takes the form of a rigid displacement $x \rightarrow x + \xi_0(y)$ with $\xi_0(y) \propto \text{Re}(\exp[ik_y y])$. Over a range of values of k_y and v_{1m} (which determines the dimensions of the hole, L and v_{2m} in Fig. 1), the perturbed tube was observed to vibrate—virtually undamped—with a frequency ω_v that increased with both k_y and v_{1m} (as in Fig. 2 below). The size of the periodic simulation domain was chosen to exclude electrostatic whistlers that could resonantly interact with the tubes. This restriction is removed in simulations of the tube-whistler interaction discussed later. A key feature of the vibrating tube observed in the simulations is the quasirigid behavior of the bounding phase-space orbits for small-amplitude vibrations, as shown in Fig. 2,

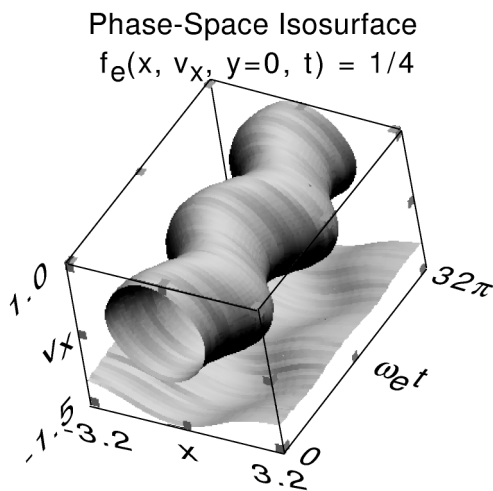


FIG. 2. Vibration of a fixed- y cross section of a phase-space tube with $v_{1m} = 2.0$ from a magnetized 2D Vlasov simulation. A rigid kink perturbation at $k_y = 0.4$ was imposed at $t = 0$. The upper passing orbit has been removed to aid visibility.

$$\pm v_1(x) \rightarrow \pm v_1(x - \xi(y, t)), \quad (4a)$$

$$\pm v_2(x) \rightarrow \pm v_2(x - \xi(y, t)) + \dot{\xi}(y, t), \quad (4b)$$

where there is no displacement in velocity for the passing orbits.

The dynamics of a phase-space tube in the highly magnetized limit are governed by the response of the electron distribution (at each y) to the perturbing electric field $\delta E_x(x, y)$. Our evaluation of the self-consistent tube dynamics in the absence of whistlers has three steps: First, determine the form of the perturbing field of a rigidly kinked tube when Eqs. (4) are valid. Next, determine the self-consistent corrections to the perturbing field due to small distortions of the orbits, which partially Debye shield the perturbing field produced by rigid displacement. Finally, determine the oscillation frequency ω_v of the trapped orbit in response to the total self-consistent perturbing field.

Based on the displaced orbits (4) seen in the simulations, we infer that the perturbed electron density $n_e(x, y)$ is (approximately) rigidly displaced from that of the unperturbed distribution by $\xi(y, t)$. We then express the perturbed potential $\phi(x, y)$ as the sum of a rigid displacement of $\phi_0(x - \xi)$ and a correction of the form $\delta \phi_P(x, y, t) \approx \xi(y, t) \delta \tilde{\phi}_P(x; k_y)$, where the subscript “ P ” signifies that the potential is a solution of Poisson’s Eq. (2) for the density in (5a) below. We also assume $\xi(y, t) \sim \text{Re}(\exp[ik_y y])$, as in our imposed initial perturbation. Thus for small displacements,

$$n_e(x) = \nabla^2 \phi(x) \approx n_{e0}(x - \xi) = \partial_x^2 \phi_0(x - \xi), \quad (5a)$$

$$\phi(x) \approx \phi_0(x - \xi) + \xi(y, t) \delta \tilde{\phi}_P(x; k_y). \quad (5b)$$

Explicitly evaluating $\nabla^2 \phi(x)$, keeping only terms linear in ξ , and subtracting $n_e(x)$ yields

$$(\partial_x^2 - k_y^2) \delta \tilde{\phi}_P(x; k_y) + k_y^2 \partial_x \phi_0(x) = 0. \quad (5c)$$

Equation (5c) has a unique solution $\delta \tilde{\phi}_P(x)$ for each k_y given $\phi_0(x)$ and the boundary conditions $\delta \tilde{\phi}_P(\pm\infty) = 0$.

A fundamental property of stationary Vlasov orbits is that the total energy (kinetic plus potential) is a constant along each orbit. Therefore, the presence of a perturbation to the BGK potential $\phi_0(x - \xi)$ must be accompanied by a deformation to the rigidly displaced orbits of (4) in order that total energy remain a constant along the bounding waterbag orbits. Specifically,

$$\frac{1}{2} (v_\alpha + \delta v_\alpha)^2 - (\phi_0 + \delta \phi) = \frac{1}{2} v_\alpha^2 - \phi_0, \quad (6)$$

where $\alpha = \{1, 2\}$ for the passing and trapped bounding orbit, respectively. The perturbing potential $\delta \phi$ in (6) is the total “self-consistent” perturbation, which will be discussed shortly. Equation (6) is an “adiabatic” approximation in that any time dependence in $\delta \phi$ is neglected. This approximation is valid for the passing orbits provided $\delta \phi$

evolves slowly compared to the time it takes an electron on the passing orbit to cross the perturbed region. For the trapped orbit, the analogous condition is that the perturbing potential changes little over the bounce period $2\pi/\omega_b$, which is consistent with frequency ordering (1). Solving Eq. (6) yields $\delta v_\alpha \approx \delta\phi/v_\alpha$. These distortions to the passing and trapped orbits will modify the potential via Debye shielding. Hence, the self-consistent perturbed potential $\delta\phi$ in (6) is the sum of the unshielded perturbation $\delta\phi_P$ and the “shielding” correction $\delta\phi_s$ due to the distortions δv_α . Since $\delta n_e = \delta v_1 - \delta v_2$ for an $f_e = 1/2$ waterbag, $\delta\tilde{\phi}_s = \delta\phi_s/\xi$ satisfies

$$\partial_x^2 \delta\tilde{\phi}_s(x) = \left[\frac{1}{v_1(x)} - \frac{1}{v_2(x)} \right] \delta\tilde{\phi}, \quad (7)$$

where we set $1/v_2(x) \equiv 0$ for $|x| \geq L$, since only v_1 contributes to the density outside the hole. Equation (7) is solved numerically for $\delta\tilde{\phi} = \delta\tilde{\phi}_P + \delta\tilde{\phi}_s$, where $\delta\tilde{\phi}_P$ is the solution to (5c). We find that the perturbations to the zero-order orbits δv_α are smaller than the dominant rigid displacements by a factor of order $(k_y L)^2$, which is a measure of deviation from rigidity. Thus, an auxiliary condition for the validity of the theory is that $k_y L \ll 1$. Despite the smallness of the orbit distortions, the corrections to $\delta\phi$ they produce can be significant, with as much as a 50% reduction in the shielded electric field perturbation.

Although we neglect the time dependence of $\delta\phi$ over a single bounce period in order to justify (6) for the trapped orbit, the fact that $\delta\phi$ is evolving cannot be ignored for longer times (i.e., many bounce periods) since an electron on the trapped bounding orbit remains continuously in contact with $\delta E_x = -\partial_x \delta\phi$. The slow evolution of the trapped orbit (and hence, of ξ) can be determined from the x integral of the second velocity moment of the Vlasov equation (3).

$$\partial_t \iint dx dv_x v_x^2 f_e = -2 \iint dx dv_x E_x v_x f_e, \quad (8)$$

which is a statement of energy conservation. For the orbit displacements of (4), Eq. (8) implies

$$A \partial_t (\dot{\xi}^2) = -2\dot{\xi} \int_{-L}^L dx v_2(x) E_x, \quad (9)$$

where A is the total cross-sectional area of the tube. Since $E_x(x) = -\partial_x \phi(x)$, it follows from (5b) and (7) that

$$\begin{aligned} E_x(x) &= -\partial_x \phi_0(x - \xi) - \xi \partial_x \delta\tilde{\phi}(x; k_y) \\ &= E_0(x - \xi) + \xi \delta\tilde{E}_x(x; k_y). \end{aligned} \quad (10a)$$

Thus, the slow evolution of ξ is governed by

$$\ddot{\xi} = -\dot{\xi} \langle \delta\tilde{E}_x \rangle = -\frac{\dot{\xi}}{A} \int_{-L}^L dx v_2(x) \delta\tilde{E}_x(x; k_y), \quad (10b)$$

since E_0 in (10a) is odd in its argument and therefore does not contribute to the right side of (9). Equation (10b)

describes tube oscillations with amplitude-independent frequency

$$\omega_v = (-\langle \delta\tilde{E}_x \rangle)^{1/2}. \quad (10c)$$

The dependence of ω_v on k_y is computed numerically and plotted in Fig. 3 for three waterbag holes with $v_{1m} = 1.1, 1.5,$ and 2.0 , together with vibration frequencies observed in our magnetized Vlasov simulations for $k_y = 0.1, 0.2,$ and 0.4 for each hole. The simulations agree with the present theory to within a few percent. The bounce frequency for the three holes, in order of increasing v_{1m} , are $\omega_b = 0.35, 0.47,$ and 0.51 , which satisfy the frequency ordering $\omega_v < \omega_b$ of (1) as required by the time-scale separation in the theory.

We now consider the interaction of a phase-space tube with a single electrostatic whistler having parallel electric field $E_w(x, y, t) = \text{Re}\{\hat{E}_w(k_x, k_y, \omega) \exp[i(k_x x + k_y y - \omega t)]\}$ where the circumflex designates an amplitude in discrete Fourier space. A resonant interaction $\omega \approx \omega_w(k_x, k_y) \approx \omega_v(k_y; L)$ requires $k_x L \ll 1$ so that $E_w(x, y, t) \approx E_w(0, y, t)$ in the vicinity of the tube. Adding this approximation of E_w to the right side of (10b), using (10c), and Fourier transforming in time yields the following forced tube response:

$$(\omega^2 - \omega_v^2) \hat{\xi}(k_y, \omega) = \hat{E}_w(k_x, k_y, \omega). \quad (11)$$

The tube-whistler coupling is closed by the influence of the oscillating field of tube, $E_T(x, y, t)$, on E_w ,

$$E_T(x, y, t) \approx E_0(x - \xi) \approx E_0(x) - \xi(y, t) \partial_x E_0(x), \quad (12)$$

where we have dropped the term proportional to ξ in (10a) and have expanded in the argument of E_0 . Only the second term in (12) contributes to the driving of whistlers since the first term is independent of y and t . The cold electron fluid equations in a highly magnetized plasma

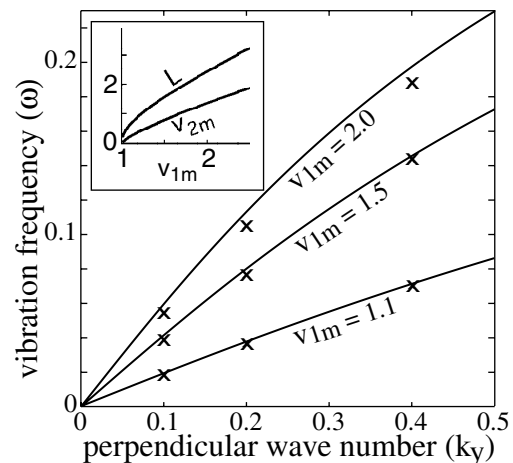


FIG. 3. Numerically determined dispersion $\omega_v(k_y)$ of tube vibrations for three BGK waterbag hole distributions (curves). The frequencies measured in Vlasov simulations are shown for three values of k_y (indicated by \times). Inset shows hole dimensions L and v_{2m} vs v_{1m} .

yield the following equation for the driven whistler field in Fourier space:

$$\begin{aligned} (\omega^2 - \omega_w^2) \hat{E}_w(k_x, k_y, \omega) &= \omega_w^2 \hat{E}_T(k_x, k_y, \omega) \\ &= -\omega_w^2 \hat{\xi}(k_y, \omega) [ik_x \hat{E}_0(k_x)]. \end{aligned} \quad (13)$$

To make contact with our periodic Vlasov and PIC simulations, we treat a single tube in a periodic domain of parallel length L_x that is a multiple of the whistler wavelength $2\pi/k_x$. Thus,

$$ik_x \hat{E}_0(k_x) = \frac{k_x^2}{L_x} \int_0^{L_x} dx e^{-ik_x x} \phi_0(x) \approx k_x^2 \frac{U_0}{L_x}, \quad (14)$$

where $U_0 = \int_{-\infty}^{\infty} dx \phi_0(x)$ is an intrinsic property of the BGK hole.

Eliminating \hat{E}_w and $\hat{\xi}$ from (11) and (13) yields the coupled dispersion relation

$$(\omega^2 - \omega_v^2)(\omega^2 - \omega_w^2) \approx -k_x^2 \omega_w^2 U_0 / L_x. \quad (15a)$$

At optimal resonance matching ($\omega = \omega_v + i\gamma$ with $\omega_v = \omega_w$ and $|\gamma| \ll \omega_w$), Eq. (15a) gives a growth rate for both whistlers and tube vibrations of

$$\frac{\gamma}{\omega_w} \approx \frac{1}{2} k_y \left(\frac{U_0}{L_x} \right)^{1/2}. \quad (15b)$$

To test the predicted growth rate of (15b), we ran our 2D magnetized Vlasov simulation in a box of dimension $L_x \times L_y$ chosen so that $\omega_w(k_{x1}, k_{y1}) \approx \omega_v(k_{y1}; L)$ where $k_{x1, y1} = 2\pi/L_{x, y}$ are the fundamental wave numbers in the periodic simulation. The simulation was “seeded” with a very low amplitude monochromatic whistler with wave vector (k_{x1}, k_{y1}) . The subsequent evolution of the electron density at fixed y is shown in Fig. 4. The growth rate is in reasonable agreement with the predicted value of $\gamma \approx 9 \times 10^{-3}$. By contrast, a comparable simulation with k_{y1} reduced by $\sim 12\%$ so as to move the interaction off resonance (with $\omega_w \approx 1.2\omega_v$) showed no sign of instability. The nonlinear saturation of the instability is evident in Fig. 4—in this case, without destruction of the tube. Simulations with multiple tubes, such as our previous PIC simulations, generally result in higher growth rates, more intense whistlers, and ultimate destruction of the tubes. Also, a quasilinear analysis is expected to show that the simultaneous growth of tube vibrations and whistlers comes

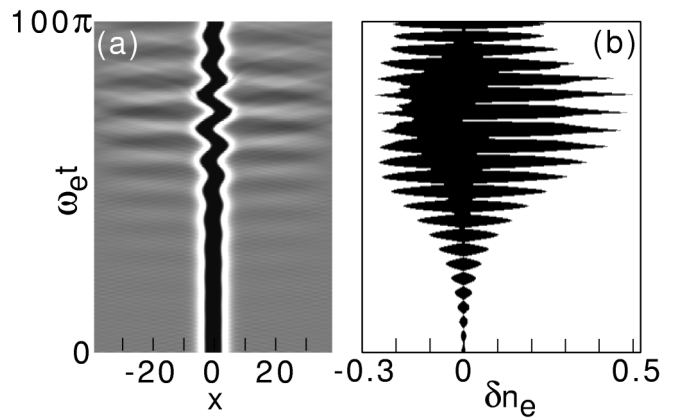


FIG. 4. Time history of electron density $n_e(x, y = 0, t)$ in Vlasov simulation of a phase-space tube interacting with a monochromatic whistler: (a) electron density; (b) x projection of density perturbation δn_e .

at the expense of energy in the unperturbed tube, which simulations show to fill in during the nonlinear phases of the instability. However, these extensions to the theory are beyond the scope of the present Letter.

We thank S. Parker, M. Oppenheim, F. Crary, and R. Ergun for helpful discussions. This research was supported by grants from NSF (ATM-9802209), NASA (NAG5-9026), and DOE (DE-FG03-98ER54502). Computations were performed at NCAR, the Advanced Computing Laboratory at LANL, and at NERSC.

*Electronic address: David.Newman@Colorado.EDU

- [1] R. E. Ergun *et al.*, *Geophys. Res. Lett.* **25**, 2025 (1998).
- [2] L. Muschietti, I. Roth, R. E. Ergun, and C. W. Carlson, *Geophys. Res. Lett.* **26**, 1093 (1999).
- [3] I. B. Bernstein, J. M. Greene, and M. D. Kruskal, *Phys. Rev. D* **108**, 546 (1957).
- [4] M. V. Goldman, M. M. Oppenheim, and D. L. Newman, *Geophys. Res. Lett.* **26**, 1821 (1999).
- [5] M. V. Goldman, D. L. Newman, F. Crary, and M. M. Oppenheim, *Phys. Plasmas* **7**, 1732 (2000).
- [6] M. M. Oppenheim, D. L. Newman, and M. V. Goldman, *Phys. Rev. Lett.* **83**, 2344 (1999).
- [7] D. L. Newman and M. V. Goldman, *Phys. Scr.* **T89**, 76 (2001).
- [8] L. Muschietti, I. Roth, C. W. Carlson, and R. E. Ergun, *Phys. Rev. Lett.* **85**, 94 (2000).
- [9] G. Vetoulis and M. Oppenheim, *Phys. Rev. Lett.* **86**, 1235 (2001).
- [10] H. L. Berk, C. E. Nielsen, and K. V. Roberts, *Phys. Fluids* **13**, 980 (1970).